Fatty acids penetration into human skin ex vivo: A TOF-SIMS analysis approach

Vytis ČižinauskasNicolas Elie and Alain BrunelleVitalis Briedis

Citation: Biointerphases **12**, 011003 (2017); doi: 10.1116/1.4977941
View online: http://dx.doi.org/10.1116/1.4977941
View Table of Contents: http://avs.scitation.org/toc/bip/12/1
Published by the American Vacuum Society

Fatty acids penetration into human skin *ex vivo*: A TOF-SIMS analysis approach

Vytis Čižinauskas[a)]
Department of Clinical Pharmacy, Lithuanian University of Health Sciences, Sukilėlių pr. 13, 50166 Kaunas, Lithuania

Nicolas Elie[b)] and Alain Brunelle[c)]
Institut de Chimie des Substances Naturelles, CNRS UPR 2301, Univ. Paris-Sud, Université Paris-Saclay, Avenue de la Terrasse, 91198 Gif-sur-Yvette, France

Vitalis Briedis[d)]
Department of Clinical Pharmacy, Lithuanian University of Health Sciences, Sukilėlių pr. 13, 50166 Kaunas, Lithuania

(Received 12 December 2016; accepted 21 February 2017; published 2 March 2017)

Linoleic, oleic, palmitoleic, palmitic, and stearic fatty acids (FAs) are commonly used in dermatological formulations. They differ by their structure, presence in the skin, and mode of application in pharmaceuticals and cosmetics compounding. These FAs are also known as chemical penetration enhancers, but their mechanisms of penetration enhancement and effect on barrier characteristics of the skin require additional study. In this study, the authors conducted an *ex vivo* analysis of the distribution of lipid components in the epidermis and dermis of human skin after applying individual FAs. The goal was to elucidate possible mechanisms of penetration enhancement and FA effects on barrier characteristics of the skin. FA penetration studies were conducted *ex vivo* on human skin and time-of-flight secondary ion mass spectrometry (TOF-SIMS) bioimaging analysis was performed to visualize and analyze distribution of FAs in skin sections. The current study demonstrated that TOF-SIMS imaging was effective in visualizing the distribution of linoleic, oleic, palmitoleic, palmitic, and stearic acid in the human skin *ex vivo* after the skin penetration experiment of individual FAs. The integration of the obtained TOF-SIMS images allowed a semiquantitative comparison of the effects induced by individual FA applications on the human skin *ex vivo*. FAs showed varying abilities to penetrate the skin and disorder the FAs within the skin, based on their structures and physicochemical properties. Linoleic acid penetrated the skin and changed the distribution of all the analyzed FAs. Skin treatment with palmitoleic or oleic acid increased the amounts of singular FAs in the skin. Penetration of saturated FAs was low, but it increased the detected amounts of linoleic acid in both skin layers. The results indicate that application of FAs on the skin surface induce redistribution of native FAs not only in the stratum corneum layer of epidermis but also in the lipid content of full epidermis and dermis layers. The results indicate that topically applied pharmaceutical products should be evaluated for potential chemical penetration enhancement and lipid component redistribution effects during formulation. [http://dx.doi.org/10.1116/1.4977941]

I. INTRODUCTION

Various approaches have been tried to achieve satisfactory penetration of drug substances through the human skin barrier. Skin is one of the most resistant barriers, as it functions to protect the human body from various external factors and interventions.[1] An efficient drug delivery system should bypass this protection such that the drug substance can penetrate sufficiently. Therefore, it is essential to understand the structure and properties of the human skin barrier.

Available scientific data show that the external epidermal layer acts as the primary permeability barrier. The outermost epidermal skin layer, called the stratum corneum (SC), consists of dead cell layers. SC is formed of corneocytes surrounded by a neutral lipid-enriched extracellular matrix.[2] The extracellular lipid matrix is formed by ceramides (CERs) 50%, cholesterol (CHOL) 25%, and free fatty acids (FFAs) 15%.[2,3] The lipid matrix is organized as stacked bilayers of fully extended CERs with CHOL molecules associated with CER sphingoid moiety and FFAs at the CER fatty acid (FA) end. Such lipid lamella organization explains the low skin permeability for water and for hydrophilic and lipophilic substances, as well as the skin barrier's resistance to environmental factors, including temperature, pressure changes, stretching, compression, bending, and shearing.[4] The integrity and functionality of the SC barrier are ensured by the presence of corneocyte envelopes, and by a ω-hydroxyceramide monolayer that surrounds corneocytes and other secreted enzymatic and structural proteins originating from lamellar bodies.[5] A secondary barrier is provided by epidermal layers below the SC.[6]

[a)]Electronic addresses: Vytis.Cizinauskas@lsmuni.lt; vytis.c@gmail.com
[b)]Electronic mail: Nicolas.Elie@cnrs.fr
[c)]Electronic mail: Alain.Brunelle@cnrs.fr
[d)]Electronic mail: Vitalis.Briedis@lsmuni.lt

Understanding skin barrier structure and composition is essential for rational design of percutaneous drug delivery systems.

Chemical and physical enhancements are applied to enhance permeation of bioactive molecules through the skin. The modification of skin barrier properties using chemical penetration enhancers (CPEs) is a widely used approach in formulation development. Nevertheless, the use of CPEs is limited due to a number of potential challenges: skin irritation and allergic reaction; difficulties in predicting and reproducing the penetration enhancement effect; pharmacological activities such as binding to the receptor sites; unintended and prolonged disturbance of the skin barrier function; possible toxicity; incompatibility with excipients and drugs; or cosmetically unacceptable sensation.[7] FAs represent a well-defined group of CPEs. They are included on the list of "generally recognized as safe substances" and are not expected to cause irritation or toxicity when used at reasonably low concentrations.[7–10] The structure and physicochemical properties of FAs make them suitable for use in pharmaceutical and cosmetic applications as multipurpose components such as emollients, thickening agents, surfactants, self-assembled vesicles, or cleansing agents.[11,12] FAs enhance skin permeability by fluidization and disorganization of SC lipids in a reversible manner.[13,14] Skin penetration studies of model drug substances suggest that unsaturated FAs (oleic, linoleic, and palmitoleic acids) have greater potential as CPEs compared to saturated FAs (palmitic or stearic acids).[7,9] Moreover, the effects of widely used linoleic and oleic FAs have been demonstrated to enhance penetration of drug molecules such as 4-aminobenzoic acid (PABA), loratadine, ketorolac tromethamine, quinupramine, tenoxicam, ondansetron hydrochloride, 5-aminolevulinic acid, and narcotic analgesics.[15–22] The most common method of analyzing skin penetration enhancement compares the permeability of a drug substance in the presence of CPE and without it to calculate the enhancement ratio. This type of analysis requires laborious sample preparation and complex analytical methods.[23] These analyses also lack sufficient data regarding how deep the components penetrate and possible effects of CPEs on epidermis and dermis barrier function.

Bioimaging mass spectrometry techniques provide simpler and more informative ways to analyze biological samples. Time-of-flight secondary ion mass spectrometry (TOF-SIMS) allows the capability to analyze the compounds in biological matrices without *a priori* knowledge of the compounds, which eliminates the need for extraction or labeling steps required by many other analytical procedures.[24–26] TOF-SIMS is particularly suitable for analyzing lipid components.[27] The applicability of the method has been confirmed by recently published results on visualization and analysis of skin penetration by drug substances roflumilast, tofacitinib, and ruxolitinib,[28] conventional antimicrobial component chlorhexidine digluconate,[29] and ZnO and TiO_2 nanoparticles.[30] The TOF-SIMS method was also applied to evaluate the penetration of tolnaftate into human skin *ex vivo* in the presence of individual FAs.[31] Additional data were provided by the application of TOF-SIMS for spatial localization of compounds of interest. The results correlated well with other analytical techniques.

In this study, the distribution of lipid components in epidermis and dermis in the human skin was analyzed *ex vivo* after the application of individual FAs. The goal was to gain a better understanding of possible mechanisms of penetration enhancement and the effects of FAs on barrier characteristics of the skin. Straight-chain saturated fatty acids (SFA) (palmitic and stearic acids), monounsaturated fatty acids (MUFA) (oleic and palmitoleic acids), and a polyunsaturated fatty acid (PUFA) (linoleic acid) were selected for penetration studies into human skin *ex vivo*. Selected SFA, MUFA, and PUFA differ by their structure, presence in the skin, and application in pharmaceuticals and cosmetics compounding. TOF-SIMS bioimaging analysis was performed to visualize and analyze distribution of FAs in human skin sections. A main goal of the study was to clarify the significance of individual components in topical products for modifying barrier properties of the skin.

II. MATERIALS AND METHODS

A. Chemicals

Polyethylene glycol 400 (PEG 400), palmitic acid (hexadecanoic acid) and linoleic acid [(9Z,12Z)-octadeca-9,12-dienoic acid] were purchased from Carl Roth GmbH (Karlsruhe, Germany). Oleic acid [(9Z)-octadec-9-enoic acid], palmitoleic acid [(9Z)-hexadec-9-enoic acid], stearic acid (octadecanoic acid), and methanol (ChromasolvW) were purchased from Sigma-Aldrich Chemie GmbH (Steinheim, Germany). Sodium azide (NaN_3) was obtained from POCh (Gliwice, Poland). Ethanol (96.3%) was obtained from Stumbras AB (Kaunas, Lithuania). All other reagents were of analytical grade.

B. Preparation of human skin

Studies with human skin were approved by Kaunas Region Bioethical Committee. Skin samples were obtained with informed consent from female patients (of age 25–40) undergoing elective abdominoplasty in the Department of Plastic and Reconstructive Surgery, Hospital of Lithuanian University of Health Sciences Kaunas Clinics. Any extraneous subcutaneous fat was removed from the dermal surface. The skin was frozen and stored at −20 °C for not longer than 6 months before use.

C. Preparation of skin penetration samples

In vitro skin penetration experiments were carried out using modified Bronaugh-type flow-through diffusion cells. The acceptor medium was circulated by a peristaltic pump (MasterflexW L/SW, Cole-Parmer Instrument Co., IL).

The donor solutions for *in vitro* skin penetration experiments were prepared by dissolving linoleic, oleic, palmitoleic, palmitic, or stearic fatty acid in PEG 400 to a concentrations of 10% (w/w). If necessary, samples were heated up to 50 °C. Clear solutions were obtained, except for palmitic and stearic

acids, each of which was semisolid at room temperature. The control skin sample was mounted without the donor solution.

Full-thickness human skin was thawed slowly, cut into small pieces, and mounted on modified Bronaugh-type flow-through diffusion cells (diffusion area 0.64 cm^2). The temperature in the block holding the cells was maintained at 37 ± 1 °C. Skin was equilibrated for 12 h by circulation of the acceptor fluid (0.9% NaCl + 0.005% NaN_3) underneath the skin. The acceptor fluid was replaced with 4 ml of fresh acceptor fluid. An infinite dose (not less than 0.2 g) of donor solutions was applied on the SC side of the skin surface for 6 h to ensure full contact of the donor phase with the skin surface and steady concentration gradient throughout the experiments. The acceptor fluid flow rate was 0.6 ml/min. After 6 h, the donor phase was carefully removed, and the skin surface was rinsed with ethanol (96.3%) and a NaCl solution (0.9%). Residual water from the samples was carefully removed with a tissue wipe. Skin specimens were immediately frozen using dry ice, wrapped in aluminum foil, and stored at −80 °C.

D. TOF-SIMS analysis

In a previous study by Kezutyte *et al.*,[31] a skin sample porosity issue was encountered. To avoid this issue, skin specimens were embedded in carboxymethyl cellulose (CMC), which has been used in mass spectrometry imaging of rice[32] and murine skin samples[33] without interference to the analysis. Briefly, a 4% CMC (average MW ∼250 000) solution was prepared. The skin samples were equilibrated in the cryostat for approximately 30 min and precut to fit the cryomolds. Later, the samples were fitted into the cryomolds, covered with a precooled CMC solution to avoid bubble formation, and snap-frozen with liquid nitrogen.

CMC-embedded skin sections of 16-μm thickness were cut in a lateral direction to the epidermis at −25 °C using a CM3050-S cryostat (Leica Microsystèmes SA, Nanterre France) and immediately deposited on a silicon wafer (2-in.-diameter polished silicon wafers, ACM, Villiers—Saint-Frédéric, France). The samples were dried under vacuum at a pressure of a few hectopascals for 15 min before the TOF-SIMS analysis. A subsequent skin section of each sample was cut and deposited on a glass slide to measure the thickness of the epidermis. A standard method of hematoxylin and eosin (H&E) staining was performed. Optical and H&E images were recorded with an Olympus BX51 microscope (Olympus, Rungis, France) equipped with lenses ×1.25 to ×50 and a motorized scanning stage (Marzhauser Wetzlar GmbH, Wetzlar, Germany) and a SC30 color camera, monitored by OLYMPUS STREAM MOTION 1.9 software. OLYMPUS STREAM MOTION software was used to measure the thickness of the epidermis in images of H&E stained samples. The thickness of the epidermis was measured at five points for each sample.

The experiments were performed using a commercial TOF-SIMS IV time-of-flight mass spectrometer (ION-TOF GmbH, Münster, Germany). The spectrometer was equipped with a liquid metal ion gun (LMIG) filled with bismuth. Bi_3^+ cluster ions were used for all experiments. Using this method, primary ions extracted from the source reached the sample surface with a kinetic energy of 25 keV and at an angle of incidence of 45°. Secondary ions are accelerated to an energy of 2 keV, fly through a field-free region, and are reflected with a single stage reflector (effective flight path ∼2 m). Then, they are postaccelerated to 10 keV just before hitting the entrance surface of the hybrid detector, which is made of one single microchannel plate, followed by a scintillator and a photomultiplier. A low-energy electron flood gun is activated between two primary ions pulses in order to neutralize the sample surface with the minimum damage.

High-current bunched mode has been used for the primary ion column operation during the experiments, providing both a beam focus of 2 μm and a pulse duration of less than 1 ns. Such experimental conditions enabled a high mass resolution, $M/\Delta M = 8000$ (full width at half maximum) at m/z 500. The Bi_3^+ primary ion current, measured at 10 kHz with a Faraday cup on the grounded sample holder, is ∼0.65 pA in the high-current bunched mode. For images of human skin sections, a large-area analysis (1.5×0.5 mm) was performed using these same LMIG conditions, and the stage scan. The number of pixels was 750×250, with each pixel having a size of 2×2 μm^2. Calibrations were conducted internally, and the signals used for initial calibration were H^-, C^-, CH^-, CH_2^-, C_2^-, C_3^-, and C_4H^-. The intensities of cholesteryl sulphate and linoleic, palmitoleic, palmitic, oleic, and stearic acids were measured using the conditions described above in negative ionization mode and expressed as ion intensity images. TOF-SIMS analysis was repeated in triplicate for each fatty acid exposed tissue in order to confirm analytical repeatability and biological reproducibility.

E. Data analysis

The data were acquired and processed using SURFACELAB version 6.2 (ION-TOF GmbH, Münster, Germany) software. Further analysis and manipulation of acquired data was carried out using ORIGIN Version 9.0 (OriginLab, Northampton, MA) software. To determine the statistical significance of the intensity changes in the skin, a nonparametric Mann–Whitney test was applied using IBM SPSS Statistics for WINDOWS, Version 20.0 (IBM Corporation, Armonk, NY). The level of significance was determined as $p < 0.05$.

III. RESULTS

A. Imaging of FAs ions in human skin *ex vivo*

TOF-SIMS analysis of human skin sections was conducted to demonstrate and evaluate the effects of FAs on the skin layers. In the TOF-SIMS images, skin sections covered an area representing not less than 1.154 mm depth from the skin surface and 0.5 mm width. The differences in sample depth were due to variable positioning of the samples. Nevertheless, this area covered the full epidermis layer, which was measured to be 0.06458 ± 0.01090 mm wide [see

supplementary material 1 (Ref. 50)] and a fragment of the dermis layer, which was 1.08942 mm wide. Depending on the part of the human body, average width of healthy human skin epidermis is up to 0.1 mm and dermis is 3–5 mm. It must be noted that the hydrophilic dermis gets swollen during the penetration studies due to the acceptor medium circulated underneath the skin, which increases the width.

The TOF-SIMS imaging area was carefully selected avoiding the shunt routes (the sebaceous glands and hair follicles containing high accumulations of lipids). TOF-SIMS images (Fig. 1) show the spatial localization of [M-H]-carboxylate ions of linoleic acid, oleic acid, palmitoleic acid, palmitic acid, and stearic acid, corresponding to the optical image obtained from the same *ex vivo* human skin sample.

The physicochemical properties of the FAs are presented in Table I. The cholesteryl sulphate (m/z 465.3044) ion is predominantly localized in the epidermal skin and was selected to show the epidermis integrity of each analyzed sample.

In order to avoid the previously described sample contamination with triglycerides during the cryosectioning procedure, the samples were cut laterally to the epidermis.[31,34] There were no visible lipid droplets in the samples, and the porosity was reduced by using the embedding procedure. However, it was noted in the microscopy images that some fragments of SC were lost during the cryosectioning procedure. The SC layer contains a large amount of lipids. Thus, the loss may have affected the detected FA intensities in upper epidermal layers.

FA spatial distribution in control skin samples, shown in Fig. 1, was detected to be in accordance with the described chemical composition of skin layers.[35] Ion intensities of unsaturated FAs were higher in the part representing the epidermis layer compared to the dermis. Ion intensities of

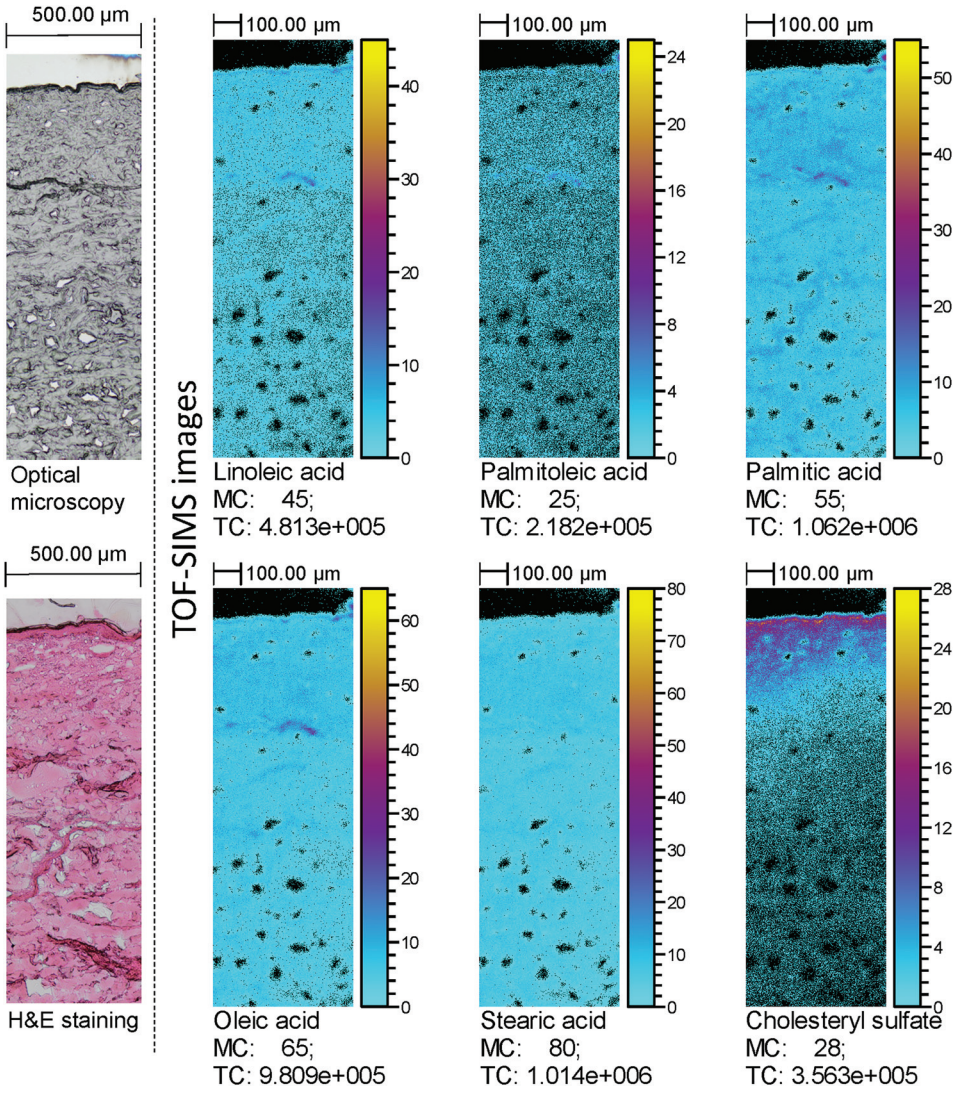

FIG. 1. TOF-SIMS images of the control skin: spatial localization of selected ions compared to the optical image. TOF-SIMS images (negative ion mode) showing lateral distribution of palmitoleic, palmitic, linoleic, oleic, and stearic acid ions in the skin. Field of view was $1.5 \times 0.5\,mm^2$, 750×250 pixels, pixel size $2 \times 2\,\mu m^2$, and fluence 5×10^{11} ions/cm^2. The amplitude of the color scale corresponds to the maximum number of counts MC and could be read as [0, MC]. TC is the total number of counts recorded for the specified m/z (the sum of counts in all pixels).

TABLE I. Physicochemical properties of the five selected FAs.

Fatty acid	Formula	Ion detected	m/z value of $[M-H]^-$ ion	logP, reported in lipidmaps	Melting point (°C)
Linoleic acid	$C_{18}H_{32}O_2$ (C18:2)	$(M-H)^-$	279.2330	5.88	−6.9
Oleic acid	$C_{18}H_{34}O_2$ (C18:1)	$(M-H)^-$	281.2486	6.11	13.4
Palmitoleic acid	$C_{16}H_{30}O_2$ (C16:1)	$(M-H)^-$	253.2173	5.33	−0.1
Palmitic acid	$C16H_{32}O_2$ (C16:0)	$(M-H)^-$	255.2330	5.55	62.5
Stearic acid	$C_{18}H_{36}O_2$ (C18:0)	$(M-H)^-$	283.2643	6.33	69.3

saturated stearic and palmitic acids were slightly higher in dermis compared to epidermis. These results, as well as the cholesteryl sulphate ions, mainly concentrated in the part representing the epidermis layer, confirm that the main structural skin layers were intact in the control skin samples. Similar spatial ion distribution was observed in samples treated with singular FAs, showing that the FA-treated samples maintained full integrity [see Fig. 2, and for all TOF-SIMS images, see supplementary material 1 (Ref. 50)].

TOF-SIMS images confirmed the integrity of the skin samples and spatial organization of FAs. However, it is difficult to compare multiple images using only color-scale bars. The quality of the samples also was affected by freezing artifacts and porosity of the skin sections appearing during the preparation of samples for TOF-SIMS analysis.

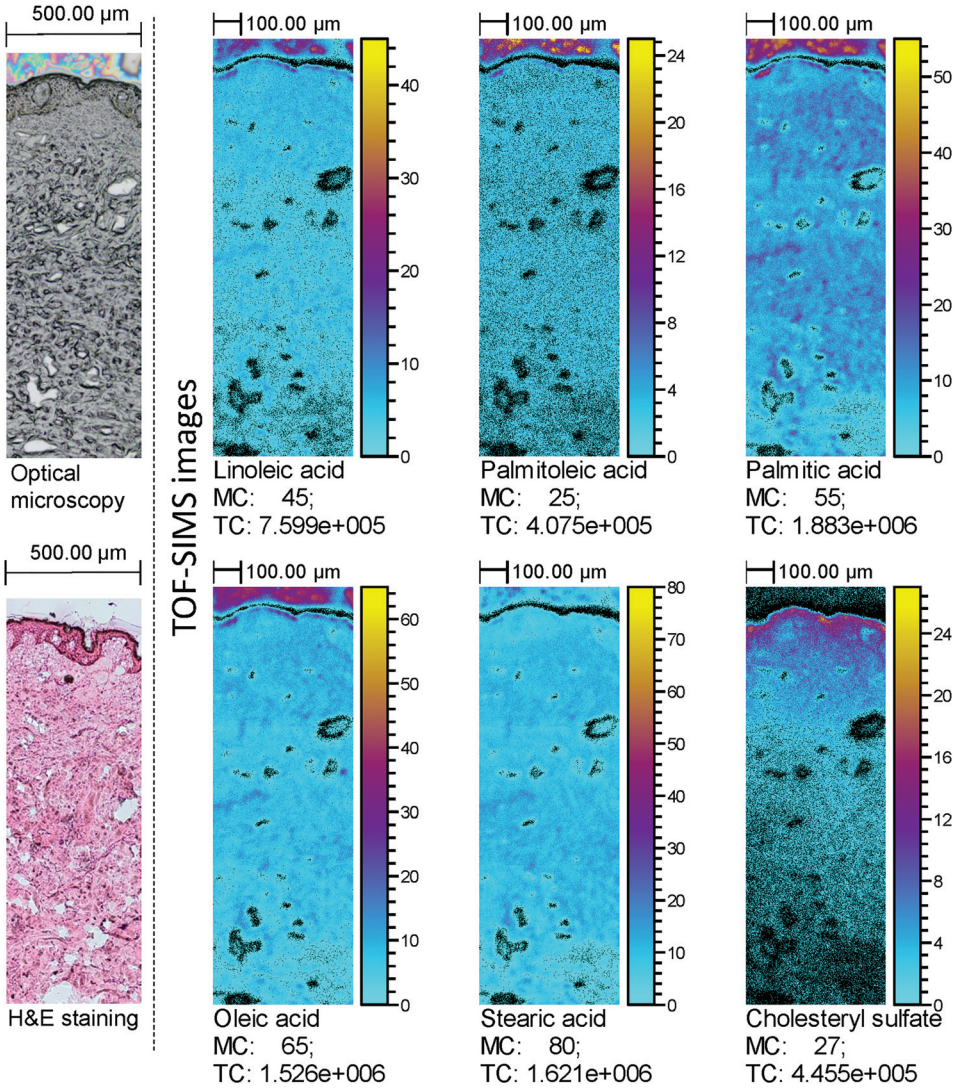

FIG. 2. TOF-SIMS images of a sample treated with linoleic acid: spatial localization of selected ions compared to the optical image. TOF-SIMS images (negative ion mode) showing lateral distribution of palmitoleic, palmitic, linoleic, oleic, and stearic acid ions in the skin. Field of view was $1.5 \times 0.5\,mm^2$, 750×250 pixels, pixel size $2 \times 2\,\mu m^2$, and fluence 5×10^{11} ions/cm^2. The amplitude of the color scale corresponds to the maximum number of counts MC and could be read as [0, MC]. TC is the total number of counts recorded for the specified m/z (the sum of counts in all pixels).

B. Analysis of FAs ion intensity profiles

To evaluate and compare the obtained ion images, each ion image was converted to intensity profiles, as a function of depth. The profiles show the detected ion intensity in the skin sample to 1.154 mm depth, and integrated over the entire width of the image (0.5 mm) (Figs. 3 and 4).

The intensity profiles provide the distribution of FAs ranging from the surface to the end of the analysis area. They allow direct comparison of ion intensities in control skin samples with the ion intensities detected in samples treated with FAs. Fluctuations were noted in the ion intensity profiles of FA-treated samples, unlike the control skin profiles.

The intensity profiles of the FAs along the depth of samples treated with linoleic acid (Fig. 3) showed increases in linoleic, palmitic, and stearic acids. In the epidermal portion of the skin, linoleic acid was detected at levels twice as high as in the control skin. The increase remained noteworthy in the dermis section, suggesting that the externally applied linoleic acid penetrated into both layers of the skin. Despite

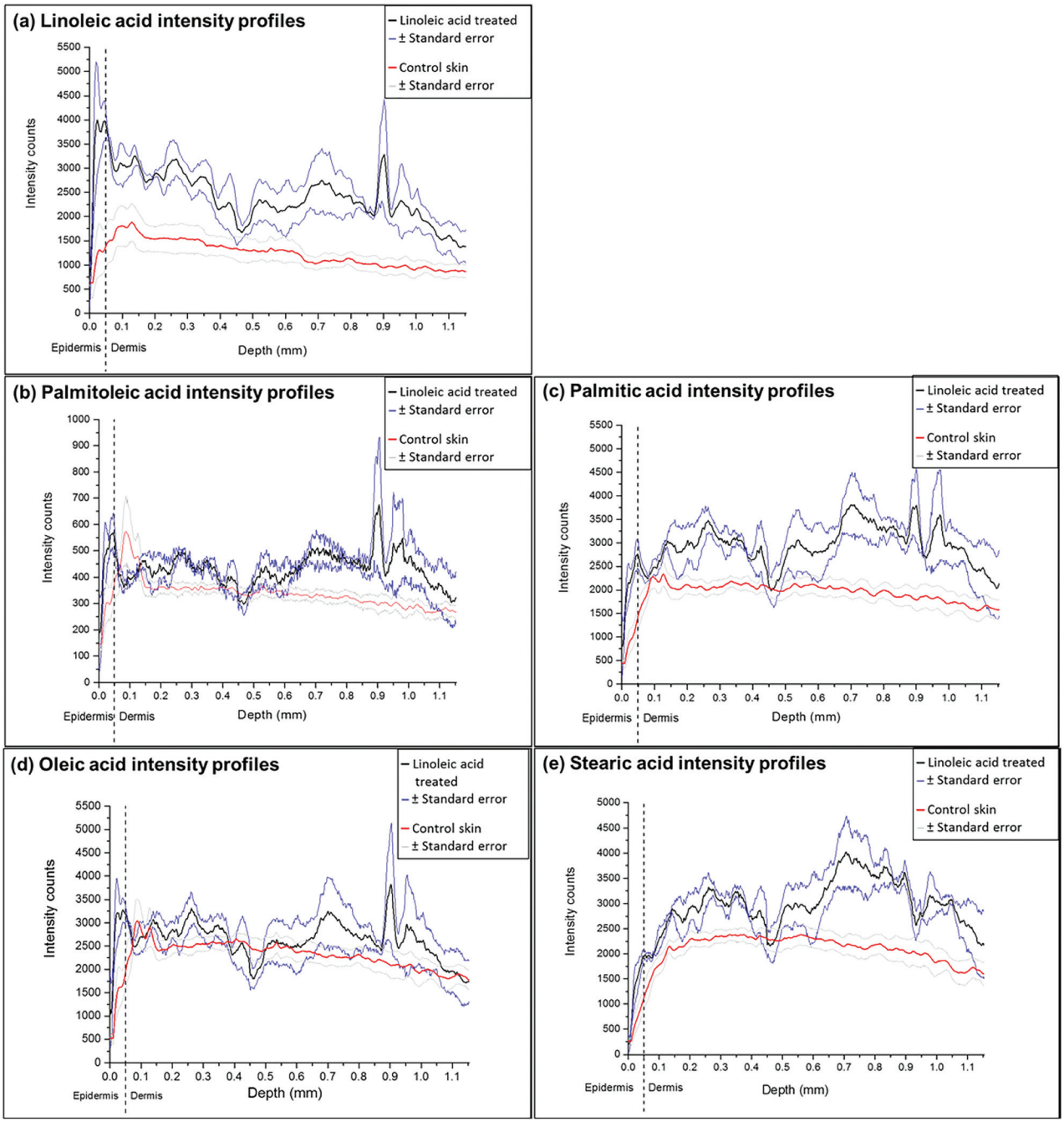

FIG. 3. Ion intensity profiles for FAs detected in samples treated with linoleic acid and compared to the intensity profiles of the control (a) linoleic acid, (b) palmitoleic acid, (c) palmitic acid, (d) oleic acid, and (e) stearic acid. The intensity profile of linoleic acid treated samples is shown as a solid black line, and solid red line indicates the control. Similar fluctuations are visible in all FA profiles.

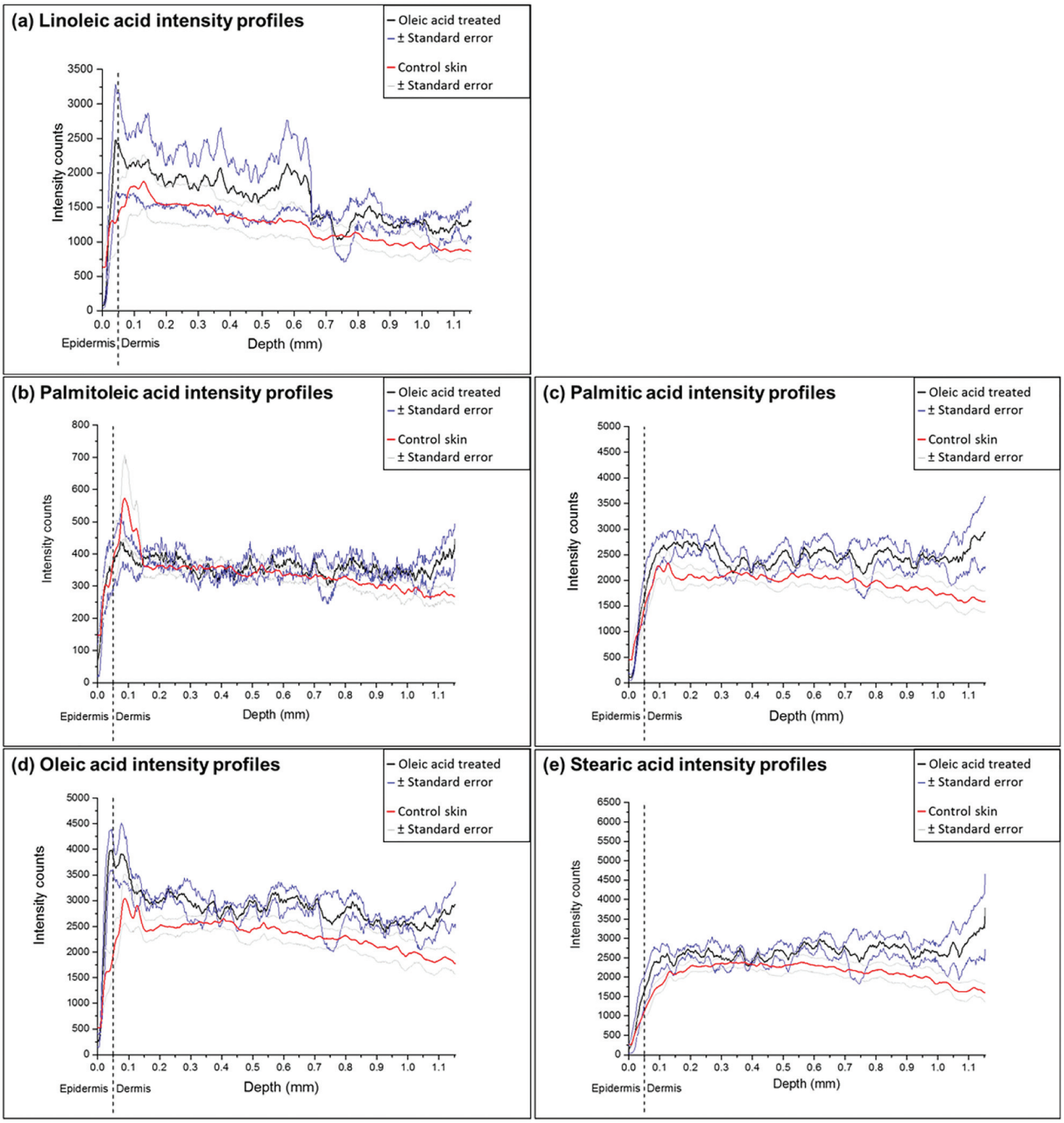

FIG. 4. Ion intensity profiles of FAs detected in samples treated with oleic acid and compared to the intensity profiles of the control: (a) Linoleic acid, (b) palmitoleic acid, (c) palmitic acid, (d) oleic acid, and (e) stearic acid. The intensity profile of linoleic acid treated samples is shown as a solid black line, and the solid red line represents the control.

the intensity changes, the shape of the profile is similar for all the FAs analyzed in the samples treated with linoleic acid, showing relatively higher intensities of FA ions in the treated sample epidermis, whereas greater amounts of palmitic and stearic acid ions were detected in the dermal layer.

The similar shapes of the intensity profiles and increase in FAs other than linoleic acid suggests that linoleic acid disorganizes the lipids in the skin, thus allowing lipids from SC to migrate into both epidermis and dermis layers with the flux of linoleic acid itself. Although the intensity profiles fluctuate more, the average values are greater, indicating the fluctuations may be caused by this disorganization.

In samples treated with oleic acid, FA ion intensity changes were less evident than in linoleic acid treated samples, as shown in Fig. 4. The amount of oleic acid was increased in all of the analyzed skin area. There was no noticeable change in palmitoleic acid ion intensity, while the amount of linoleic acid was increased from the surface down to 0.6 mm depth, where it reached a peak intensity, and then decreased to the control level in the deeper skin region.

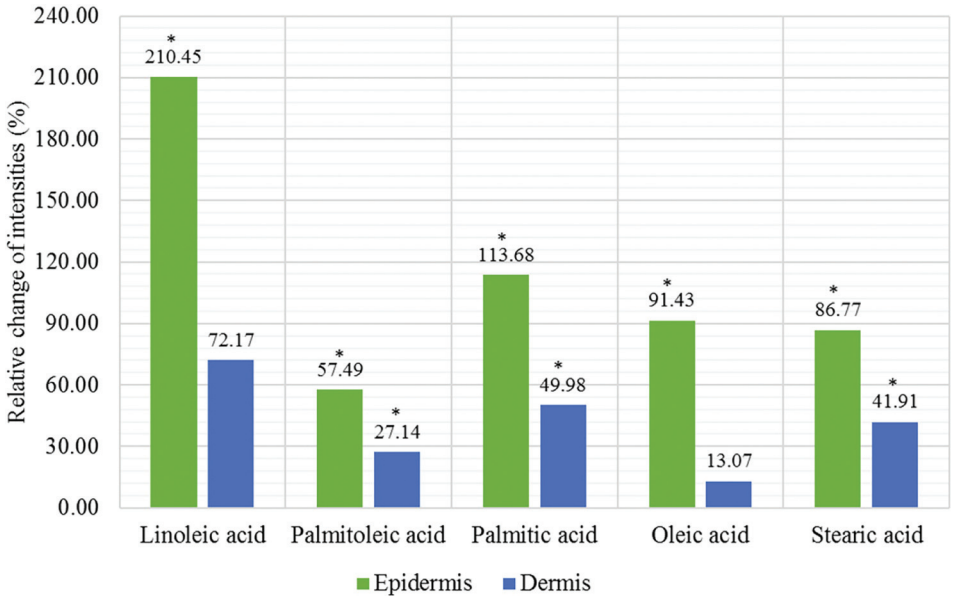

FIG. 5. Comparison of linoleic acid induced changes to control skin samples of human skin *ex vivo*. The bars represent the percentage changes in intensities detected in the epidermis of linoleic acid treated samples and compared to the control. Green bars represent the changes in epidermis and blue bars represent the changes in dermis. Statistically significant changes are marked *, $p < 0.05$.

Palmitic and stearic acid profiles were similar: showing a small increase in epidermis and upper part of dermis, then further increasing sharply in the depth ranging from 0.6 to 1.154 mm from the surface of the skin.

These results show that oleic acid permeates the skin through the epidermis and dermis. Moreover, it disorganizes other FAs, including linoleic, stearic, and palmitic acids, which are detected in high intensities in the skin.

The ion intensity profiles of the samples treated with other FAs [see supplementary material 2 (Ref. 50) for all fatty acids intensity profiles, as a function of depth] showed that the treatment of skin with palmitoleic acid resulted in an increase of palmitoleic acid in the epidermis only, while in the samples treated with palmitic and stearic acid, a noticeable increase in linoleic acid was detected.

The ion intensity profiles provided reliable information showing significant changes at each depth point of the sample, but for obtaining a quantifiable comparison of the profiles they were further integrated.

C. Semiquantification of the changes and comparison to the control samples

Intensity profiles were subdivided into two areas corresponding to epidermis (0–0.06458 mm) and dermis (0.06458–1.154 mm), based on the average of measured epidermis thicknesses. Areas under the intensity profile were integrated and normalized dividing it by the depth in millimeters, obtaining a unit corresponding to intensity counts per 1 mm of analyzed depth. The FA intensity values per 1 mm of analyzed depth in epidermis and dermis were used to obtain a semiquantitative analysis approach of the results, as well as to compare the effects of different individual FAs to the control skin samples. A previous study by Bich *et al.* reported on a semiquantitative lipid analysis using TOF-SIMS.[36] A nonparametric Mann–Whitney test was selected for the statistical comparisons and the level of significance was $p < 0.05$.

Data integration and statistical comparison facilitated an objective evaluation of observed FA distribution changes. Significant changes were detected in all analyzed FAs in epidermis of skin samples subjected to the application of linoleic acid. This confirmed that linoleic acid disorganizes all of the analyzed FAs in the epidermis layer (Fig. 5). In the dermis, statistically significant changes of palmitoleic and stearic acid were detected. Thus, a 72% increase in linoleic acid remained insignificant because of the linoleic acid variation in between the samples.

In the samples treated with the remaining FAs, significant effects were detected only for singular FAs detected in the skin (Table II). Comparison of oleic acid treated samples to the control skin, shown in Fig. 6, revealed a significant accumulation of oleic acid in epidermis (86%) and dermis (22%),

TABLE II. Statistically significant changes in FA distribution following treatment with selected FAs. Changes in FA concentration detected among skin treatments and control sample are represented as the names of FAs: LA, linoleic acid; OA, oleic acid; POA, palmitoleic acid; PA, palmitic acid; and SA, stearic acid. N/D, no statistically significant difference.

	Significant changes of FAs distribution	
Skin treatment	Epidermis	Dermis
Linoleic acid	LA, POA, OA, PA, SA	POA, PA, SA
Oleic acid	OA	OA
Palmitoleic acid	POA	N/D
Palmitic acid	LA	LA
Stearic acid	N/D	SA

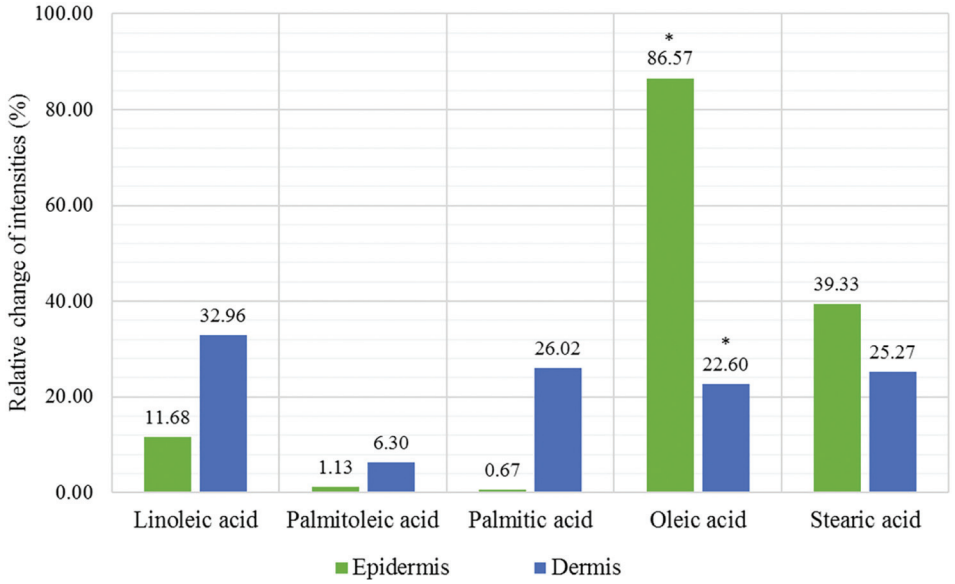

FIG. 6. Comparison of oleic acid induced changes to control skin samples of human skin *ex vivo*. Bars represent the percentage changes in intensities detected in epidermis of oleic acid treated samples and compared to the control. Green bars represent the changes in epidermis and blue bars represent the changes in dermis. Statistically significant changes are marked *, $p < 0.05$.

confirming that oleic acid passes the epidermal barrier. There were no statistically significant changes in other FAs analyzed, showing that oleic acid did not influence their distribution in the skin.

Analysis of palmitoleic acid treated samples exhibited a significant increase in palmitoleic acid of up to 179% compared to the control skin in the epidermal section. No changes were detected in the dermal layer, demonstrating that palmitoleic acid does not pass the epidermal barrier.

An increase in linoleic acid was noted in the intensity profiles of samples treated with saturated palmitic and stearic FAs. However, the increase was significant only in the palmitic acid treated samples: 176% in epidermis and 113% in dermis. After the application of stearic acid, an increase of linoleic acid up to 94% in the epidermis and 93% in the dermis remained insignificant. The quantity of linoleic acid varies among the samples, resulting in decreased ability to detect the statistically significant changes. Thus, the effects of the increased linoleic acid amounts following application of saturated FAs are associated with skin occlusion improving the penetration of other compounds.

After the application of stearic acid, a minor but statistically significant stearic acid increase of 30% was detected in the dermis. This change could be attributed to the increased mobility of linoleic acid. In contrast, the increase in linoleic acid was greater following the application of palmitic acid, but the 55% increase of palmitic acid in the epidermis remained statistically insignificant. This shows that evaluation reliability of the changes in FA distribution highly depends on the variation of a particular FA concentration in the skin samples.

IV. DISCUSSION

TOF-SIMS analysis of individual FAs in the human skin samples *ex vivo* after the 6 h penetration studies allowed a comparison of how FAs affect the naturally present FA distribution in the skin. Human skin samples used in the comparative study were from the same donor, thus minimizing the effects of interindividual variations. Integration of the ion intensities in the TOF-SIMS images and the subsequent statistical analysis enabled evaluation of the effect of each FA and a comparative analysis.

As it was noted in the work of Kezutyte *et al.*,[31] TOF-SIMS analysis of the skin samples may have been affected by a number of factors. It is recognized that the analyzed FAs are naturally present on the skin surface due to products from hydrolysis of sebaceous lipids to C16 or C18 MUFA and PUFA.[34,37] To minimize these influences, skin surfaces were cleaned with 0.9% NaCl prior to *in vitro* experiments. In addition, after *in vitro* experiments, the donor phase was carefully removed, followed by rinsing with ethanol and 0.9% NaCl, to eliminate the traces of sebum from the skin surface.

Other potential factors we considered were sample contamination with triglycerides and porosity appearing during the cryosectioning of the skin. No visible lipid droplets were detected in the samples, and the porosity in the sections was decreased compared to complementary data from the published human skin *ex vivo* analysis.[31] As the possibility of sample contamination with triglycerides during the cryosectioning procedure remains questionable, the samples were cut in a direction parallel to the epidermis.[31,34]

The procedure for freezing skin sample freezing following the FA skin penetration experiment also may have decreased the quality of cryosections. To prevent contamination of skin samples with additional substances, we avoided using any additional freezing media and froze the samples with dry ice. This freezing method increased the porosity of the samples, due to ice formation in the tissue, but as no

additional compounds were used in the freezing procedure, the only freezing artifacts were the porosity of the samples. Optical microscopy images showed that fragments of SC were lost during the embedding and cryosectioning procedure. This loss may have affected the amounts of FAs detected in the upper epidermal layer, which explains the excessive amounts of FAs detected in the skin after the application of individual FAs compared to control. These drawbacks in sample preparation also may have caused increased variation in FA distribution between the samples.

Despite the partial loss of SC during the sample preparation, integration of obtained TOF-SIMS images supported a semiquantitative approach and statistical comparison of the acquired data. The effects induced by applying individual FAs on human skin *ex vivo* were evaluated in terms of FA concentrations detected in epidermal and dermal layers. Statistical comparisons provided additional information about the significance of changes to concentrations of FAs in human skin caused by application of individual FAs. These comparisons also clarified the effects of different FAs on the skin.

A characteristic feature of FAs applied on the skin is their ability to modify the mobility of molecules in the skin. Ibrahim and Li[14] showed that the effectiveness of a CPE in enhancing transdermal permeation along the lipoidal pathway across SC is related to enhancer solubility and amount in the SC lipids. A general relationship exists between the enhancer effect and octanol–water partition coefficient.[38] It should be noted that according to regular solution theory, the lower a material's melting point, the greater its solubility in a given solvent. All analyzed FAs have similar logP values, but the melting points of saturated FAs are higher when compared to unsaturated FAs, thus limiting their solubility in skin lipids (Table I). Analysis of the samples individually treated with stearic or palmitic acid demonstrated minor or insignificant increases of these FAs in epidermis or dermis layers. In the current study, palmitic acid did not pass the SC barrier, while a minor increase in stearic acid was noted in the dermis. Also, both FAs increased the amounts of linoleic acid in human skin *ex vivo* epidermis and dermis layers. This effect is related to skin occlusion, which improves the penetration of other compounds. Statistical analysis of the induced changes demonstrated that variation in concentration of a particular FA in the skin samples is a critical factor.

The ability of saturated FAs to enhance penetration of donepezil was determined to be comparable to that of unsaturated FAs.[39] Palmitoleic acid, which is a C16 alkyl chain MUFA, was demonstrated to be an efficient penetration enhancer of naloxone, compared to C16 and C18 alkyl chain saturated and unsaturated FAs.[10] A significant increase in palmitoleic acid was noted in the epidermis with no reliable increase in dermis and no changes in distribution of other FAs. These results indicate a limited ability of palmitoleic acid to pass the epidermis-dermis barrier and suggest that it can be used for drug delivery systems when it is necessary to increase permeation of a compound into the epidermis.

Linoleic acid induced redistribution of FAs within the human skin *ex vivo*. Linoleic acid is a polyunsaturated omega-6 essential FA, having two *cis* unsaturated double bonds at C9 and C12 locations, and has the lowest melting point of the analyzed FAs. Linoleic acid is an established CPE and typically used in comparison to oleic acid. It has been confirmed that linoleic acid penetrates the skin more rapidly than oleic acid.[40] This suggests that linoleic acid should exhibit greater penetration enhancement properties, and this has been confirmed by studies with PABA, loratadine, ketorolac tromethamine, and quinupramine.[16–19] In a study of oxymorphone, hydromorphone and morphine skin penetration, the penetration enhancement effect of linoleic acid was correlated to its concentration.[15] Lipid disorganization by the linoleic acid in the SC as well as in total skin could be attributed to higher fluidity of lipid regions, resulting in increased permeation of the penetrants. Increased skin lipid bilayer fluidity after the application of oleic and linoleic acid has been confirmed in a FT-IR study.[41] Despite the higher disorganization of the lipids in the SC induced by linoleic acid, the MUFA oleic acid increased the permeation of tenoxicam, ondasetrone hydrochloride, carvedilol, and 5-aminolevulinic acid.[20,22,42]

Using the lipid protein partitioning theory, which describes the mechanisms of action for various CPE classes, oleic acid was chosen as one of the model CPEs.[43] The *cis* double bond at C9 of oleic acid provides the potential for a kink structure formation in molecules and can disrupt the ordered skin lipids. It has been suggested that oleic acid melts the lipid chain fragment within the bilayer structure, together with some nonpolar material. It also breaks associations between lipid polar groups and disrupts cholesterol-stiffened regions, thereby increasing their fluidity.[13,43] Various approaches have been used to assess oleic acid effects on SC lipids, confirming the previous theory and demonstrating the ability of oleic acid to disrupt the SC barrier by incorporating itself into the lipid lamellae causing increased disordering of the alkyl chain.[44–49] In the current study, the oleic acid concentration increased in both skin layers, while no disordering of other analyzed FAs was detected. These observations show that oleic acid permeates both skin layers without disordering other analyzed FAs in the skin, and also participates in the formation of regions with increased fluidity.

V. CONCLUSIONS

TOF-SIMS imaging is an informative technique for analyzing the penetration of substances naturally present in the skin. It provides the ability to analyze the distribution of several selected compounds simultaneously. The current study showed that TOF-SIMS imaging can be applied in visualizing the distribution of linoleic, oleic, palmitoleic, palmitic, and stearic acids in the human skin *ex vivo* after skin penetration by individual FAs. The integration of the obtained TOF-SIMS images allows semiquantitative comparison of the effects induced by applying individual FAs on the human skin *ex vivo*.

Linoleic, oleic, palmitoleic, palmitic, and stearic FAs are commonly used in dermatological formulations. They showed different abilities to penetrate the skin and disorder the FAs within the skin depending on their structure and physicochemical properties. Linoleic acid penetrated the skin and changed the distribution of all the analyzed FAs, while other individual FAs did not induce similar changes. Skin treatment with palmitoleic or oleic acid increased the amounts of singular FAs in the skin. Penetration of saturated FAs was low, but it increased the detected amounts of linoleic acid in both skin layers. The results indicated that application of FAs on the skin surface induces redistribution of native FAs not only in the SC but also in the lipid content of full epidermis and dermis layers. Possible chemical penetration enhancement and lipid component redistribution effects should be evaluated while formulating topically applied pharmaceutical products.

ACKNOWLEDGMENTS

The authors wish to thank Embassy of France in Lithuania for supporting this research.

[1]K. Madison, J. Invest. Dermatol. **121**, 231 (2003).
[2]K. R. Feingold, J. Lipid Res. **48**, 2531 (2007).
[3]J. van Smeden, M. Janssens, G. S. Gooris, and J. A. Bouwstra, Biochim. Biophys. Acta—Mol. Cell Biol. Lipids **1841**, 295 (2014).
[4]I. Iwai *et al*., J. Invest. Dermatol. **132**, 2215 (2012).
[5]P. M. Elias, J. Invest. Dermatol. **132**, 2131 (2012).
[6]P. Fomby and A. J. Cherlin, Pharm. Res. **30**, 1099 (2013).
[7]A. C. Williams and B. W. Barry, Adv. Drug Delivery Rev. **64**, 128 (2012).
[8]L. B. Lopes, M. T. J. Garcia, M. Vitoria, L. B. Bentley, and M. V. L. B. Bentley, Ther. Delivery **6**, 1053 (2015).
[9]M. E. Lane, Int. J. Pharm. **447**, 12 (2013).
[10]B. J. Aungst, Pharm. Res. **6**, 244 (1989).
[11]S. A. Ibrahim and S. K. Li, Pharm. Res. **27**, 115 (2010).
[12]L. Kumar, S. Verma, S. Kumar, D. N. Prasad, and A. K. Jain, Artif. Cells, Nanomed., Biotechnol. **45**, 251 (2016).
[13]B. W. Barry, J. Controlled Release **6**, 85 (1987).
[14]S. A. Ibrahim and S. K. Li, Int. J. Pharm. **383**, 89 (2010).
[15]M. Mahjour, B. E. Mauser, and M. B. Fawzi, Int. J. Pharm. **56**, 1 (1989).
[16]H. Tanojo, J. A. Bouwstra, H. E. Junginger, and H. E. Bodde, Pharm. Res. **14**, 42 (1997).
[17]C. W. Cho and S. C. Shin, Int. J. Pharm. **287**, 67 (2004).
[18]Y. A. Cho and H. S. Gwak, Drug Dev. Ind. Pharm. **30**, 557 (2004).
[19]S. C. Shin, J. Kim, W. J. Kim, S. J. Kim, and C. W. Cho, Pharm. Dev. Technol. **12**, 429 (2007).
[20]H. S. Gwak, I. S. Oh, and I. K. Chun, Drug Dev. Ind. Pharm. **30**, 187 (2004).
[21]H. S. Gwak and I. K. Chun, Int. J. Pharm. **236**, 57 (2002).
[22]M. B. R. Pierre, E. Ricci, A. C. Tedesco, and M. V. L. B. Bentley, Pharm. Res. **23**, 360 (2006).
[23]T. Kezutyte, T. Drevinskas, A. Maruska, R. Rimdeika, and V. Briedis, Acta Pol. Pharm. **68**, 965 (2011), available at http://www.ptfarm.pl/pub/File/Acta_Poloniae/2011/6/965.pdf.
[24]T. Leefmann, C. Heim, S. Siljeström, M. Blumenberg, P. Sjövall, and V. Thiel, Rapid Commun. Mass Spectrom. **27**, 565 (2013).
[25]T. Leefmann, C. Heim, A. Kryvenda, S. Siljeström, P. Sjövall, and V. Thiel, Org. Geochem. **57**, 23 (2013).
[26]P.-L. Lee, B.-C. Chen, G. Gollavelli, S.-Y. Shen, Y.-S. Yin, S.-L. Lei, C.-L. Jhang, W.-R. Lee, and Y.-C. Ling, J. Hazard. Mater. **277**, 3 (2014).
[27]M. L. Kraft and H. A. Klitzing, Biochim. Biophys. Acta **1841**, 1108 (2014).
[28]P. Sjövall *et al*., Anal. Chem. **86**, 3443 (2014).
[29]A. M. Judd, D. J. Scurr, J. R. Heylings, K.-W. Wan, and G. P. Moss, Pharm. Res. **30**, 1896 (2013).
[30]N. A. Monteiro-Riviere, K. Wiench, R. Landsiedel, S. Schulte, A. O. Inman, and J. E. Riviere, Toxicol. Sci. **123**, 264 (2011).
[31]T. Kezutyte, N. Desbenoit, A. Brunelle, and V. Briedis, Biointerphases **8**, 3 (2013).
[32]N. Zaima, N. Goto-Inoue, T. Hayasaka, and M. Setou, Rapid Commun. Mass Spectrom. **24**, 2723 (2010).
[33]N. Goto-Inoue, T. Hayasaka, N. Zaima, K. Nakajima, W. M. Holleran, S. Sano, Y. Uchida, and M. Setou, PLoS One **7**, e49519 (2012).
[34]L. Norlén, I. Plasencia, and L. Bagatolli, Int. J. Cosmet. Sci. **30**, 391 (2008).
[35]M. Boncheva, Int. J. Cosmet. Sci. **36**, 505 (2014).
[36]C. Bich, D. Touboul, and A. Brunelle, Int. J. Mass Spectrom. **337**, 43 (2013).
[37]J. van Smeden, W. A. Boiten, T. Hankemeier, R. Rissmann, J. A. Bouwstra, and R. J. Vreeken, Biochim. Biophys. Acta **1841**, 70 (2014).
[38]S. A. Ibrahim and S. K. Li, J. Pharm. Sci. **98**, 926 (2009).
[39]J. Choi, M. K. Choi, S. Chong, S. J. Chung, C. K. Shim, and D. D. Kim, Int. J. Pharm. **422**, 83 (2012).
[40]E. O. Butcher, J. Invest. Dermatol. **21**, 43 (1953).
[41]V. B. Nair and R. Panchagnula, Pharmacol. Res. **47**, 563 (2003).
[42]S. Amin, K. Kohli, R. K. Khar, S. R. Mir, and K. K. Pillai, Pharm. Dev. Technol. **13**, 533 (2008).
[43]B. W. Barry, Int. J. Cosmet. Sci. **10**, 281 (1988).
[44]V. H. Mak, R. O. Potts, and R. H. Guy, Pharm. Res. **7**, 835 (1990).
[45]A. C. Rowat, N. Kitson, and J. L. Thewalt, Int. J. Pharm. **307**, 225 (2006).
[46]T. N. Engelbrecht, A. Schroeter, T. Hauss, and R. H. H. Neubert, Biochim. Biophys. Acta **1808**, 2798 (2011).
[47]A. Ruettinger, M. A. Kiselev, T. Hauss, S. Dante, A. M. Balagurov, and R. H. H. Neubert, Eur. Biophys. J. **37**, 759 (2008).
[48]D. Kessner, M. A. Kiselev, T. Hauss, S. Dante, S. Wartewig, and R. H. H. Neubert, Eur. Biophys. J. **37**, 1051 (2008).
[49]M. A. Kiselev, N. Y. Ryabova, A. M. Balagurov, S. Dante, T. Hauss, J. Zbytovska, S. Wartewig, and R. H. H. Neubert, Eur. Biophys. J. **34**, 1030 (2005).
[50]See supplementary material at http://dx.doi.org/10.1116/1.4977941 for TOF-SIMS images, epidermis measurements and ion intensity profiles of all the samples treated with fatty-acids.